Click to view poster

[EA]The Role of Forward Seismic Modeling: Outcrop Analogs of Deep-Water Architectures*

Jamie K. Pringle[1] and David A. Stanbrook[2]

Search and Discovery Article #51679 (2020)**
Posted September 28, 2020

*Adapted from extended abstract prepared in conjunction with poster presentation given at 2008 International Conference and Exhibition, Cape Town, South Africa, October 26-29, 2008
 DOI:10.1306/51679Pringle2020

[1]School of Physical Sciences & Geography, Keele University, Keele, United Kingdom
[2]Maersk Olie og Gas A/S, Copenhagen, Denmark (Stan_Stanbrook@murphyoilcorp.com)

Abstract

Geometric and architectural information from appropriately selected outcrop analogues can be extremely valuable in building subsurface geologic models. Geologists need to assess and distil key outcrop data for comparison with seismic, petrophysical, and other sub-surface information. However, even high-resolution seismic does not approach typical outcrop scales, so how does the geologist bridge the gap?

Forward Seismic Modelling (also known as synthetic seismic) is one approach. This involves the collation of outcrop data in the form of large-scale photomontages which are then interpreted and ground-truthed by high-resolution, 1D sedimentary log data. Hand-held petrophysical tools (e.g. a gamma-ray spectrometer) may also be utilized for sub-surface comparison. The detailed architectural interpretation is then imported into specialist software that convolves the model, using user-specified seismic acoustic impedance contrasts and central frequency (Ricker) wavelets. Impedance contrasts can be calculated using published velocity and density values for different lithologies and allows the geoscientist to vary values to simulate the petroleum reservoir they are interested in. The seismic frequency can also be varied to simulate the depth and/or quality of seismic available.

Presented here are two modelled examples of key turbidite architectural geometries: 1) the Chalufy Onlap, Grès d'Annot, SE France, and 2) the Ainsa II Channel Complex, Campodarbe Group, N Spain. A suite of forward seismic models are shown with dominant seismic frequencies and rock values typical of Gulf of Mexico and UK North Sea reservoirs.

Introduction

Onlapping stratigraphy and turbidite channels are of common interest in hydrocarbon exploration as potential reservoirs. Stratigraphic traps in confined, deep-water basins are often dependent on relationships between deep-water strata and the basin slopes. Deep-water strata typically

onlap the confined basin margin, but precise onlap relationships can be difficult to resolve, particularly in salt provinces where salt margins are often steep and difficult to seismically resolve. Important details of onlap relationships may be obscured, leading to uncertainty concerning reservoir charge and seal. Turbidite channel-fill traps, on the other hand, may range from high net:gross, sheet-like geometries, multiple channel re-incisions to mass-transport complexes or passive infill. Seismic data sets may not adequately resolve these internal channel geometries. Interpreting the architectural complexity will be crucial in predicting fluid flow behaviour in analogous subsurface reservoirs. However internal architectures and overall net:gross can be hard to resolve in typical seismic datasets. In these circumstances well-exposed outcrop examples can provide insights into the seismic expression of onlap relationships and channel architectures.

Forward seismic models of large-scale, outcrop exposures have been generated by other authors (Batzle and Gardner, 2000; Coleman et al., 2000; Bourgeois et al., 2004; Schwab et al., 2007) to allow both geologists and geophysicists to compare high-resolution outcrop data and seismic data from comparable reservoir intervals. In this study, two outcrop exposures - one an onlap and the other a channel complex - has been field investigated, interpreted, digitized, and modelled to generate forward seismic 2D sections.

The Montagne de Chalufy turbidite onlap in the Haute Provence Region of the French Alps is a spectacular, seismic-scale exposure of an onlap surface which has been well documented and can be usefully converted to a synthetic seismic section. The Ainsa II channel within the Campodarbe Group in northern Spain is a large-scale exposure of slope conduits. The channel complex consists of five stacked channel units, characterized by distinct internal architectures is well documented and can be usefully converted to a synthetic seismic section.

The Chalufy Onlap and Interpretation

This is a well-known and documented onlap (Elliott et al., 1985; Apps, 1987; Sinclair 1994; Hilton and Pickering 1995; Pickering and Hilton, 1998; Joseph and Ravenne, 2001; Smith and Joseph, 2004; Puigdefàbregas et al., 2004) and offers a seismic scale onlap surface at the contact of basin-floor Marnes Bleues with the Marnes Brunes Inférieures/Grès d'Annot turbidites. Positioned at the distal end of the exposed Grès d'Annot turbidite system the section is at the proximal end of the Trois Evêchés sub-basin with sediments being fed from the Grand Coyer sub-Basin to the north. An 800 m long, 150 m high section of the onlap surface is considered in this work (Figure C1).

Four turbidite sandstone bodies are exposed in this sector of the onlap surface. The Grès d'Annot sandstone bodies, separated by units of brown shale and thin-bedded turbidites (Marnes Brunes Inférieures), apparently onlap towards the south-southeast (Figure C1). The observed relationship is complicated by a fault that results in a repetition of the onlap of the middle sandstone body to apparently represent three sandstone bodies (see Puigdefàbregas et al., 2004).

The lower-most sand body (SB1) is up to 35 m thick and contains, in the lower and upper part, thick-bedded, graded and massive sandstones interpreted as the deposits of high-density turbidity currents. The middle part of SB1 is more shale-rich and consists of thinner-bedded, lower density, Bouma-type turbidites. This sector of the onlap is relatively steep and sandstone beds in SB1 retain their thickness in close proximity to the slope with beds onlapping the surface abruptly and terminating over a distance of 1-2 m (Figure C2).

The second sandbody (SB2) is 10-12 m thick and onlaps a more gently dipping sector of the onlap surface. The thickness of the sandstone body is retained across the exposure, but then thins gradually for 120 m before terminating against the onlap surface. The final termination is abrupt and again involves the final bed-base rising steeply against the onlap surface. The lower part of SB2 comprises coarser-grained, high density turbidites with inversely graded lower divisions that correspond with the traction carpet layers of Lowe (1982, Figure C2). The upper part of this body is dominated by a large-scale slump fold (Joseph and Ravenne, 2001; Smith and Joseph, 2004).

In sectors where the onlap surface is a contact between the Marnes Bleues and the Marnes Brunes Inférieures (the later vertically separating the sandstone bodies), the contact is cryptic by comparison. Blue-grey marls with slightly varying carbonate content (Marnes Bleues) are abruptly but cryptically overlain by marls with lower carbonate content and thin, cm-scale turbidite sandstone beds that become thicker and more common upwards.

The Montagne de Chalufy outcrop had initially been field investigated and interpreted as a 2-D cross-section (with adjustment for photomontage perspective). Two sedimentary interpretations were investigated (Pringle, 2003); a complete model retaining observed faults and heterolithic intervals, and a simple model with both the structural complexities and the heterolithic detail removed. The more detailed model is shown here: with both turbidite thin-bedded intervals within the sand-rich intervals and structural (fault) complications preserved over the four onlapping (including the onlap repetition as a result of the faulting), un-deformed, massive sandstone bodies (Figure C3).

The Ainsa II Channel and Interpretation

The Ainsa II Channel is within the well-studied Eocene Campodarbe Group (see Clark, 1995; Pickering and Corregidor, 2000; Pringle et al., 2001, Larue et al., 2004; Schwab et al., 2007) which crops out in the southern part of the Central Pyrenees. In the central sector of the Tremp-Pamplona Basin, near the town of Ainsa, the Campodarbe Group consists of fine-grained, submarine slope sediments (characterized by mud-rich mass-failure deposits) and coarse-grained, sand-rich channel and scour-fill deposits. One of the largest exposures of these slope conduits is the Ainsa II Channel Complex. The channel complex consists of five stacked channel units, each of which is characterized by a distinctive internal architecture (Clark, 1995; Figure A1).

A study of the Ainsa II Complex has made possible a detailed interpretation of the sedimentological aspects of the channel complex, both as a whole, and as individual channels; the section is shown with five times vertical exaggeration in Figure A2 (cf Figure A1). The dominant palaeoflow is northwest to west-northwest, thus the exposure is an oblique section of the channel intervals. The major erosive down-cutting surfaces show lateral shifting of channelized intervals to the south, here numbering five. Lateral accretion features can be seen in Channel 1, and the base of Channel 2. Channel 3 also shows thalweg deposits. Channel margin onlap relationships can clearly be seen in channel 4, and the steep arcuate margin of Channel 5 has been interpreted as a rotational slide or slump scar element.

From the detailed bed correlation shown in Figure A2 and combined with the photomontage interpretation shown in Figure A1, a generalized sedimentary input model of the Ainsa II Complex was constructed (Figure A3; Pringle, 2003). The described facies have been grouped into four types: i) massive sandstone units (and minor discontinuous shales) that were typically 1 m thick; ii) medium-bedded sandstones (typically

0.5 m thick) and shales; iii) predominantly shale and thin (typically 0.1 m) sandstones; and iv) shale intervals. Acoustic rock-properties (Figure A4) have been assigned to each of the facies groups and used for the construction of the synthetic seismic images.

Method

Forward Seismic Modelling (also known as synthetic seismic) in these studies involves the collation of outcrop data in the form of large-scale photomontages that are then interpreted to produce a detailed, 2D architectural interpretation of the outcrop exposure. The initial interpretation is then validated by both field ground-truth investigations and detailed sedimentary outcrop logs that also provide high-resolution, 1D data. The detailed architectural interpretation and the chosen dominant seismic wavelet frequency is then fed into specialist software that convolves the model into a seismic section, using user-input and seismic impedance contrasts between different lithologies. Seismic impedance contrast can then be calculated using published velocity and density values for the different lithological types in the selected section, enabling the rock values to be varied in order to simulate the petroleum reservoir under consideration. The geoscientist can also vary the frequency to simulate the depth and/or quality of seismic available.

Modelling Strategy

The interpreted outcrop models were subsequently digitized and then processed using the GMAplus STRUCT™ software program. A number of parameters were tested; the simplest being the potential vertical seismic resolution differences that would be produced using different dominant frequencies. The modelling program expects average velocity and density values for each bedding unit. It was decided to use velocity values from producing reservoirs, as the aim was to simulate conventional seismic information through reservoirs with comparable seismic impedance values (Figure C4 and Figure A4). Three sets of parameters were varied; the seismic impedance contrast, the resolution that could be seen from the input sedimentary model, and different dominant wavelet frequencies.

Seismic Impedance Contrast

In both the Chalufy Onlap and Ainsa II Channel models typical velocity and density values were taken from published data for: i) massive sandstone units (and minor discontinuous shales); ii) medium-bedded, sandstones and shales; iii) predominantly shale and thin sandstones and lastly; iv) shale intervals. As the aim was to simulate conventional seismic information through reservoirs with comparable seismic impedance values, velocity values from producing reservoirs were used. The producing fields were the Magnus Field, a Jurassic, North Sea (UKCS) reservoir and the Mars Field, a Plio-Pleistocene, Gulf of Mexico reservoir. Values for the three reservoirs were obtained from published data from Partington (1993) and Chapin (1996) respectively.

Wavelet Frequency

Four dominant Ricker wavelet frequencies were used in these studies: 26 Hz wavelet, typical of seismic datasets from deeper buried reservoirs; 52 Hz wavelet, typical of industry higher-frequency shallow seismic datasets; 78 Hz wavelet, selected as current, cutting-edge seismic acquisition and; 104 Hz wavelet, sometimes acquired for investigating the near-surface placement of oil rigs. The GMAplus STRUCT™

software program displays both the seismic image and the seismic traces overlain on the time-converted, seismic model. Traces are spaced at 12.5 m, equivalent to typical inline seismic section. Vertical incidence, zero-offset rays were chosen to avoid the complexities of dip move-out and migration, which commonly occur in standard, seismic Common Mid-Point (CMP) data.

For the Chalufy Model the underlying Cretaceous Basement values used were constant for all models, checked against Badley (1948) values for similar lithologies. Although the underlying Marnes Bleues Formation was observed to be dominantly composed of marls, it was decided to model these units as fast-shales as may be seen as in the geological record in areas of with long periods of non-clastic deposition.

Results of the Chalufy Onlap Model

Figure C5 shows two synthetic seismic sections, generated using 26 and 52 Hz dominant frequency wavelet based on the detailed interpretation using lithological parameters of a Plio-Pleistocene Gulf of Mexico analogue (the Mars Field). Figure C6 shows two synthetic seismic sections, generated using 26 and 52 Hz dominant frequency wavelet based on the detailed interpretation using lithological parameters of a Jurassic North Sea analogue (the Magnus Field). The brightest amplitudes (and hence largest impedance contrasts) were found in models representing the Jurassic North Sea reservoirs. However overall variations in impedance values seem to have little effect on results at the high Signal:Noise Ratios (SNR) used (Noise was not added to any of the models). The massive sandstone bodies of the Grès d'Annot could be identified on all sections, at both high and low frequencies. At the higher frequency (50 Hz), the variations in sandstone body thickness could also be resolved. The small thrust offset could be distinguished in all high frequency synthetic sections. Note that such a high frequency (50 Hz) signal would not normally be returned from deep Jurassic targets in the North Sea. The Jurassic North Sea reservoir parameters show high velocity values, and hence a tighter synthetic seismic section; comparison of time values for the Cretaceous basement in Figure C5 with Figure C6 shows a TWT of 0.28 and 0.25, respectively.

Results of the Ainsa II Channel Model

Low Resolution Seismic Images (26 Hz) are shown in Figure A5 and Figure A6. The lowest frequency wavelets chosen (26 Hz) are typically used for imaging deep reservoir targets, such as the Jurassic turbidite reservoirs in the North Sea. For both reservoir scenarios, an extra broad positive amplitude reflection event is present in the middle part of the section, compared to the background values, with the slumped interval to the left of the section not able to be imaged. The acoustic rock properties from the three different reservoirs do, however, show subtle differences. The lowest impedance contrast between heterogeneities within the channel complex comes from the Jurassic North Sea analogue. At the low-resolution seismic frequency, the thickening of the top reflector and the slump scar feature would indicate the likely presence of complex reservoir architecture.

High Resolution Seismic Images (52 Hz) are shown in Figures A5 and Figure A6. Higher frequencies (e.g. 52 Hz) are commonly used for imaging higher level reservoir targets. Using this frequency, a greater amount of reservoir architecture can be interpreted. As well as the obvious positive amplitude event in the middle part of the section, some heterogeneities are resolved at this interval. The image suggests there are at least three compartments to the channel complex: one corresponding to channel units 1, 2, and 3; one to channel unit 4; and one to the slump scar and infill, channel unit 5.

Very High Resolution Seismic Images (78 Hz) are shown in Figures A5 and Figure A6. Current shallow level, seismic targets are imaged up to 78 Hz, this third frequency chosen to generate seismic sections. Some additional internal channel heterogeneity can be resolved using this frequency, especially channels 2-4, with channel 4 being successfully resolved. The geophysical interpretation using this frequency data would be close to the digitized input sedimentary model.

The differing impedance values for the chosen reservoir examples had little effect on the interpretation at the high signal:noise ratios used. Although some of the internal sedimentary architecture is resolved, the impedance values from Jurassic North Sea reservoir analogue yield the highest amplitudes from the generated synthetic sections.

Discussion

Analysis of the Chalufy Onlap synthetic seismic section shows that resolving onlapping sandstone units on seismic sections is a potential problem. Using typical seismic frequencies of 26 Hz, only the large-scale, sand-rich intervals could be successfully differentiated from the background materials. The onlap relationship of these bodies onto palaeo-slopes and other potentially topographically complex basin-floors could not be recognized or resolved, which is crucial when defining stratigraphic traps. The internal, sand-poor heterolithic intervals were also not well resolved, which may make petroleum geologists over-estimate potential reserves. In the Chalufy Onlap model the higher 52 Hz frequency data produced much improved vertical and horizontal seismic resolution, with both the heterolithics intervals and the major fault imaged, although the small faults were not resolvable. The Gulf of Mexico has a relatively shallow stratigraphic depth (Figure C5), whereas the Jurassic North Sea analogue showed the poorest resolution as would be expected from a deeper reservoir (Figure C6).

The overall appearance of the Chalufy onlap surface is imaged effectively in the synthetic seismic data in that the presence of the sandstone bodies, their onlapping nature and the major fault locally offsetting the onlap sandstone bodies are visible in each case. The thickness contrast between SB1 and SB2 is successfully imaged in all cases, and the abrupt termination of SB1 contrasting with the more gradual thinning of SB2 is also apparent in most cases.

The results of the Ainsa II Channel study suggest that a 2D synthetic seismic section generated from low frequency (26 Hz) wavelet would most probably give a geophysical interpretation that would miss the sedimentary heterogeneity that may well be present within a turbidite channel-complex that may be crucial for fluid-flow behaviour. These low frequencies are those typically used in deep Jurassic targets in the North Sea. With a 52 Hz frequency however, typically used in shallow level Tertiary targets, a much-improved geophysical interpretation could be achieved that would resolve the major architectural elements of a stacked, channel sequence. However, the relatively thin intervals that could potentially form the barriers to fluid flow would not be imaged. The nature of channel stacking, erosional contacts or mud drapes would, most likely, not be imaged at this frequency.

Conclusion

Sedimentological and structural data, observed in the field by geoscientists working on outcrop analogues, often give far higher resolution than is observed in conventional seismic data. Similarly, what looks like relatively simple sedimentology and structural data to the geophysicist can,

in fact, be a lot more complicated and is not being imaged. Large-scale outcrops can be usefully forward seismic modelled to compare the high resolution of geo-scientific data from outcrops to the relatively lower resolution from seismic data.

Seismic sections generated from low frequency (26 Hz) wavelet are not likely to resolve critical sedimentary heterogeneities that may well be present within a turbidite sequences that may represent fluid-flow barriers, baffles, or conduits. Higher (52 Hz) frequencies found in shallower targets have the potential to resolve the major architectural elements though the relatively thin intervals that could potentially form barriers or conduits to fluid flow would still not be imaged.

An improvement to this modelling exercise would be adding seismic ‘noise’ to make the 2D sections more realistic and to utilize the collected 1D sedimentary logs to create more realistic seismic wavelets between the different modelled sedimentary intervals. Further work should generate fully 3D cubes to be relevant to modern, seismic industry data and be re-run with differing quantities of fluids to be more realistic. Overburden should also be added to make the seismic models more comparable to producing reservoirs. Forward modelling of the synthetic seismic images could be also be undertaken to compare and contrast the similarities between the 'synthetic geology' from the original geological interpretation that was the basis of the input model.

Acknowledgments

Peter Olden gave guidance on GMA™ software. Robin Westerman and Leon Barens related the convolutional model used by GMA to the wider context of wavefield modelling and of surface seismic acquisition and processing. The Heriot-Watt University Genetic Units Project (GUP) and GEOTipe Project, both funded by petroleum-industry consortia, are acknowledged for financial support for J. Pringle. Will Schweller, and Chuck Stelting are thanked for attendance on a Chevron internal fieldtrip to the Ainsa area.

References Cited

Apps, G., 1987, Evolution of the Grès d'Annot Basin, SW Alps: PhD Thesis, University of Liverpool, 451 p.

Badley, M.E., 1948, Practical Seismic Interpretation, Boston, USA, 266 p.

Batzle, M., and M.H. Gardner, 2000, Lithology and Fluids: Seismic Models of the Brushy Canyon Formation, West Texas, *in* A.H. Bouma and C.G. Stone (eds.), Fine Grained Turbidite Systems: American Association of Petroleum Geologists Memoir 72, p. 127-142.

Bourgeois, A., P. Joseph, and J-C. Lecomte, 2004, Three Dimensional Full Wave Seismic Modelling Versus One Dimensional Convolution: The Seismic Appearance of the Grès d’Annot Turbidite System, *in* P. Joseph and S. Lomas (eds.), Deep-Water Sedimentation in the Alpine Foreland Basin of SE France: New Perspectives on the Grès d'Annot and Related Systems: Geological Society, London, Special Publication, 221, p. 401-417.

Chapin, M.A., G.M. Tiller, and M.J. Mahaffie, 1996, 3-D Architecture Modelling Using High-Resolution Seismic Data and Sparse Well Control: Examples from the Mars “Pink” Reservoir, Mississippi Canyon Area, Gulf of Mexico, *in* P. Joseph and S. Lomas (eds.), Applications of 3-D Seismic Data to Exploration and Production: American Association of Petroleum Geologists Studies in Geology No. 42, p. 123-131.

Clark, J.D, 1995, Detailed Section Across the Ainsa II Channel Complex, South Central Pyrenees, Spain, *in* K.T. Pickering, R.N. Hiscott, N.HI. Kenyon, and R.D.A. Smith (eds.), Atlas of Deep-Water Environments: Architectural Style in Turbidite Systems: Chapman & Hall, London, p. 139-144.

Coleman, J.L., F.C. Sheppard III, and T.K. Jones, 2000, Seismic Resolution of Submarine Channel Architecture as Indicated by Outcrop Analogues *in* A.H. Bouma and C.G. Stone, (eds.), Fine-Grained Turbidite Systems: American Association of Petroleum Geologists Memoir 72, p. 119-126.

Elliott, T., G. Apps, H. Davies, M. Evans, G. Ghibaudo, and R.H. Graham, 1985, A Structural and Sedimentological Traverse Through the Tertiary Foreland Basin of the External Alps of Southeast France, *in* P.A. Allen and P. Homewood (eds.), Field Excursions Guidebook for the International Association of Sedimentologists Meeting on Foreland Basins, Fribourg, p. 39-73.

Hilton, V.C., and K.T. Pickering, 1995, The Montagne de Chalufy Turbidite Onlap, Eocene-Oligocene Turbidite Sheet System, Hautes Provençe, SE France, *in* K.T. Pickering, R.N. Hiscott, N.HI. Kenyon, and R.D.A. Smith (eds.), Atlas of Deep-Water Environments: Architectural Style in Turbidite Systems: Chapman & Hall, London, p. 236-241.

Joseph, P., and C. Ravenne, 2001, (Excursion D) Chalufy, *in* P. Joseph and S. Lomas (eds.), Turbidite Sedimentation in Confined Settings: Research Meeting and Field Excursion to the Grès d’Annot, Nice, France, 10-15 September 2001.

Larue, D., 2004, Outcrop and Waterflood Simulation Modeling of the 100-Foot Channel Complex, Texas and the Ainsa II Channel Complex, Spain: Analogs to Multistory and Multilateral Channelized Slope Reservoirs, *in* M. Gramer, P.M. Harris, G.P. Eberli (eds.), Integration of Outcrop and Modern Analogs in Reservoir Modeling: American Association of Petroleum Geologists Memoir 80, p. 337-364.

Lowe, D.R., 1982, Sediment Gravity Flows: II. Depositional Models with Special Reference to the Deposits of High-Density Turbidity Currents: Journal of Sedimentology, v. 52, p. 279-297.

Partington, M.A., P. Copestake, B.C. Mitchener, and J.R. Underhill, 1993, Genetic Sequence Stratigraphy for the North Sea Late Jurassic and Early Cretaceous: Distribution and Prediction of Kimmeridgian-Late Ryazanian Reservoirs, *in* J.R. Parker (ed.), The North Sea and Adjacent Areas: Petroleum Geology of Northwest Europe, Proceedings of the 4th Conference, The Geological Society, London, 1, p. 347-370.

Pickering, K.T., and J. Corregidor, 2000, 3D Reservoir Scale Study of the Eocene Confined Submarine Fans, South Central Spanish Pyrenees: 20th Annual Bob F. Perkins GCSSEPM Foundation Research Conference, p. 776-781.

Pickering, K.T., and V.C. Hilton, 1998, Turbidite Systems of Southeast France: Vallis Press, London, 229 p.

Pringle, J.K., 2003, Integrated Techniques for the Acquisition and Visulaisation of 3D Meso- to Macro-Scale Sedimentary Architectures of Petroleum Reservoir Outcrop Analogues: PhD Thesis, Institute of Petroleum Engineering, HeriotWatt University, Edinburgh, UK, 326 p.

Pringle, J.K., J.D. Clark, A.R. Westerman, D.A. Stanbrook, A.R. Gardiner, and B.E.F. Morgan, 2001, Virtual Outcrops: 3-D Reservoir Analogues, *in* L. Ailleres and T. Rawling (eds.), Animations in Geology: Journal of the Virtual Explorer, p. 3.

Pringle, J.K., D.A. Stanbrook, and J.D. Clark, 2008, Resolving Deep-Water Channel Architectures: High-Resolution Forward Seismic Modelling of Turbidite Systems, Ainsa II Channel, Campodarbe Group, Northern Spain, *in* K. Schofield et al. (eds.), Answering the Challenges of Production from Deep-Water Reservoirs: Analogues and Case Histories to Aid a New Generation: GCSSEPM 28th Annual Bob F. Perkins Conference Proceedings, Houston, USA, December 7-9th, 20 p.

Puigdefàbregas, C., J. Gjelberg, and M. Vaksdal, 2004, The Grès d'Annot in the Annot Syncline: Outer Basin-Margin Onlap and Associated Soft-Sediment Deformation, *in* P. Joseph and S. Lomas (eds.), Deep-Water Sedimentation in the Alpine Foreland Basin of SE France: New Perspectives on the Grès d'Annot and Related Systems: Geological Society, London, Special Publication, 221, p. 367-388.

Schwab, A.M., B.T. Cronin, and H. Ferreira, 2007, Seismic Expression of Channel Outcrops: Offset Stacked Versus Amalgamated Channel Systems: Marine and Petroleum Geology, v. 24, p. 504-514.

Sinclair, H.D., 1994, The Influence of Lateral Basin Slopes on Turbidite Sedimentation in the Annot Sandstones of SE France: Journal of Sedimentary Research, v. A64, p. 42-54.

Smith, R., and P. Joseph, 2004, Onlap Stratal Architectures in the Grès d'Annot: Geometric Models and Controlling Factors, *in* P. Joseph and S. Lomas (eds.), Deep-Water Sedimentation in the Alpine Foreland Basin of SE France: New Perspectives on the Grès d'Annot and Related Systems: Geological Society, London, Special Publication, 221, p. 389-399.

Stanbrook, D.A., J.K. Pringle, T. Elliott, J.D. Clark, and A. Gardiner, 2008, Resolving Deep-Water Stratigraphic Traps: Forward Seismic Modelling of a Turbidite Onlap; Montagne de Chalufy, Grès d'Annot Formation, SE France, *in* K. Schofield et al. (eds.), Answering the Challenges of Production from Deep-water Reservoirs: Analogues and Case Histories to Aid a New Generation: GCSSEPM 28th Annual Bob F. Perkins Conference Proceedings, Houston, USA, December 7-9th, 23 p. doi:10.13140/RG.2.1.3005.2241

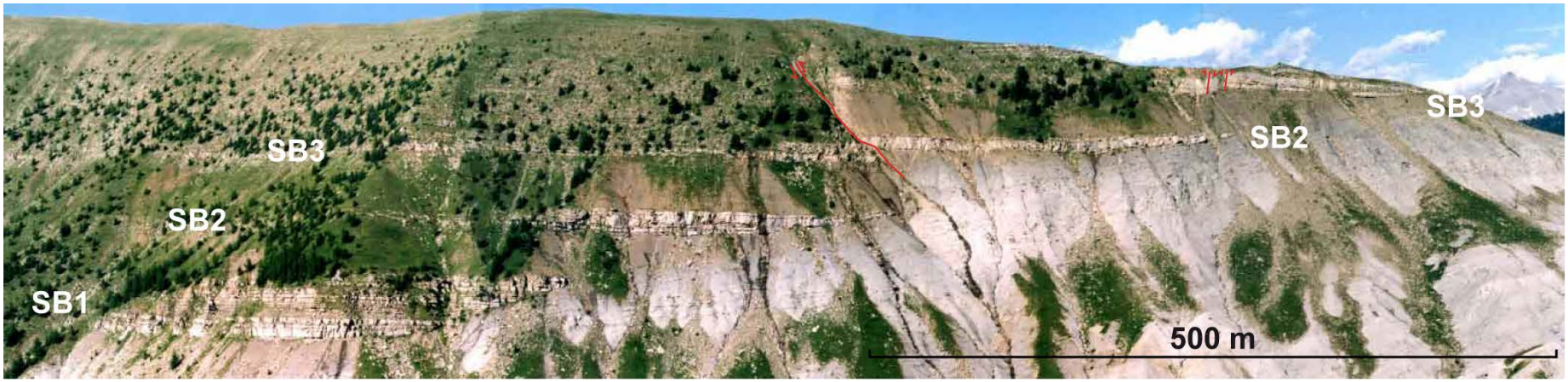

Figure C1. The Montagne de Chalufy onlap section; the foreland basin into which the Grès d'Annot was deposited had a complex basin-floor topography, which controlled the distribution of sand-bodies. Note the onlap of sandstone packets within the Grès d'Annot onto the Marnes Bleues slope. The Geometry is complicated by oblique-slip faults, causing repetition of the middle sandbody onlap on both sides of the main fault (annotated).

Figure C2. Left: Final, abrupt termination of Sandstone Body 2 against the onlap surface. Note the abrupt rise of the basal erosion surface. Right: Inverse grading produced in a traction carpet layer at the base of a high density turbidite sandstone bed in the lower part of Sandstone Body 2.

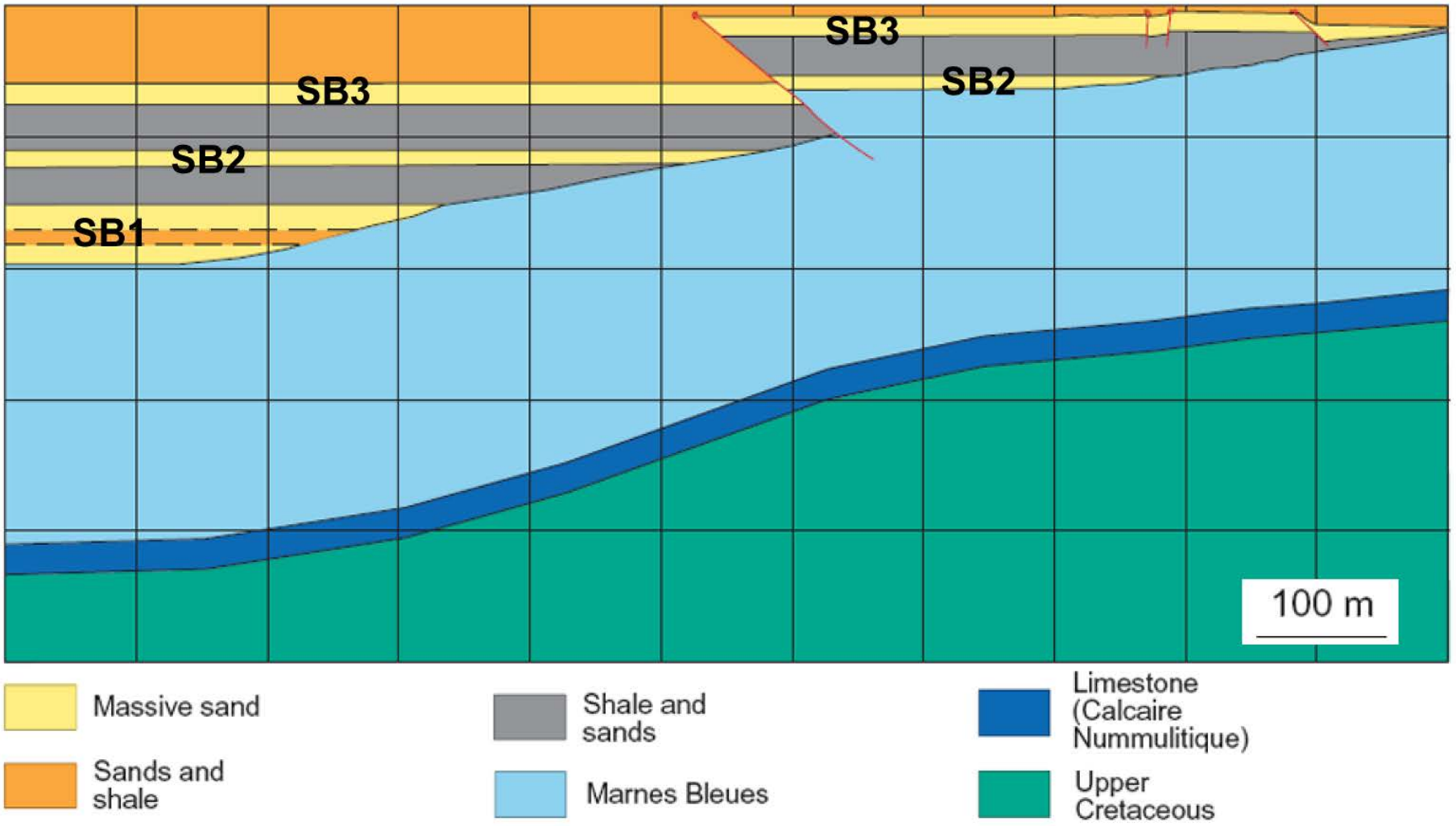

Figure C3. Detailed 2D input model showing both structural interpretation and thin-bedded heterolithics present within the sand-rich intervals (representing the Marnes Brunes Inférieures and Grès d'Annot facies respectively). Note the scale is the same for zxy.

Gulf of Mexico Parameters

	Velocity (m/s)	Density (g/cc)	Impedance (kg m^{-2} s^{-1})
Massive Sand	3672	2.08	7628 x 10^3
Shale and Marl	2650	2.25	5692 x 10^3
Interbedded sands & shales	3387	2.13	7214 x 10^3

Jurassic North Sea Parameters

	Velocity (m/s)	Density (g/cc)	Impedance (kg m^{-2} s^{-1})
Massive Sand	4233	2.43	10286 x 10^3
Shale and Marl	3110	2.53	7868 x 10^3
Interbedded sands & shales	3858	2.48	9568 x 10^3

Figure C4. Seismic parameters from producing fields used in this study to represent the different formations associated with the onlap.

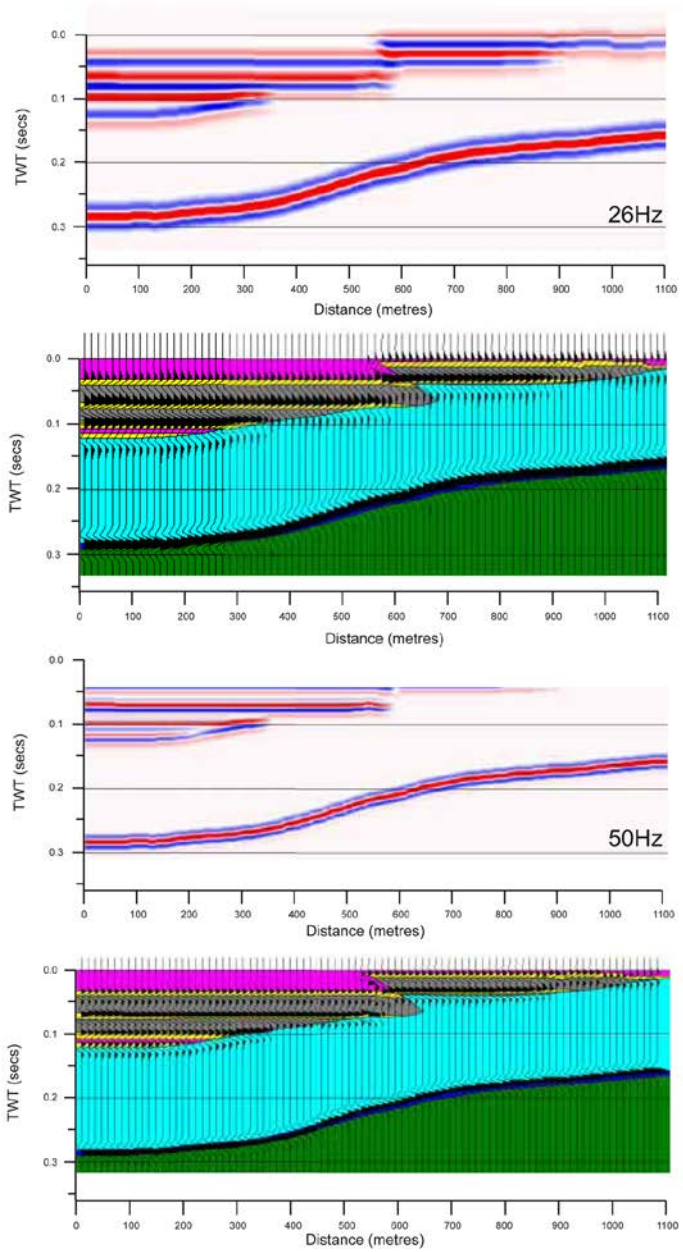

Figure C5. Detailed model Plio-Pleistocene Gulf of Mexico analogue output from GMAplus STRUCT™ software showing (A/B) 26 Hz and (C/D) 52 Hz frequencies, showing color impedance and wiggle trace wavelets, respectively. Note wavelet sections have interpreted model shown behind as solid colors.

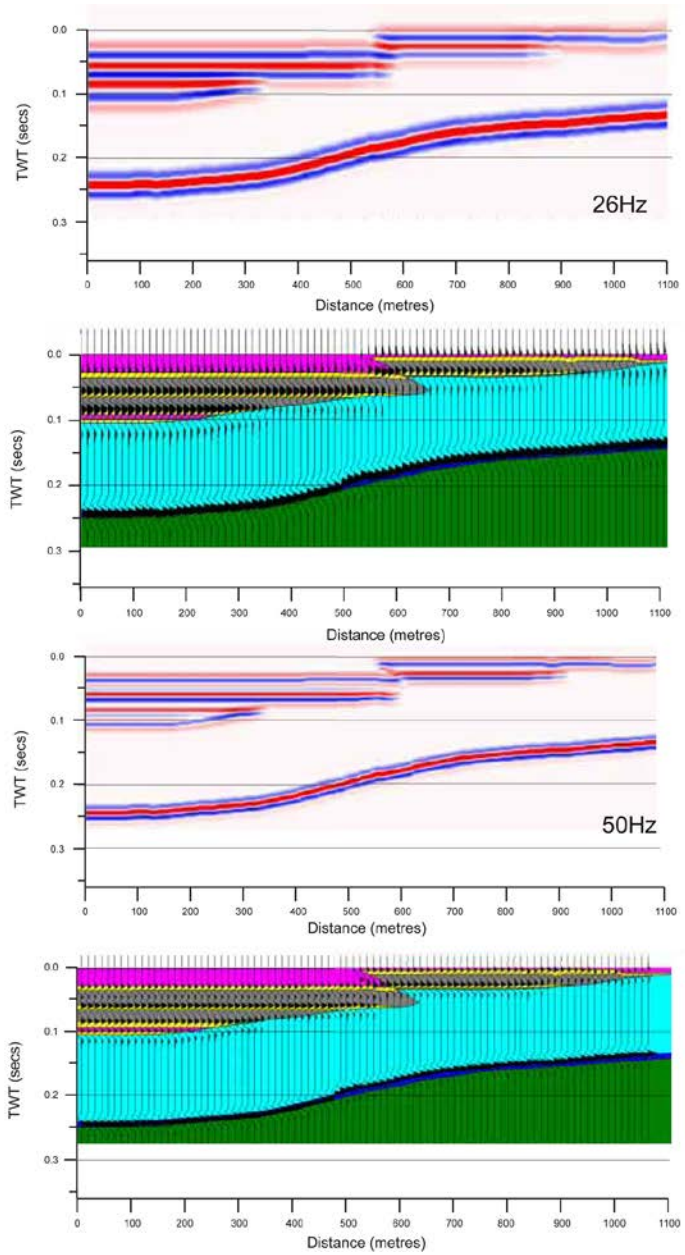

Figure C6. Detailed model Jurassic North Sea analogue output from GMAplus STRUCT™ software showing (A/B) 26 Hz and (C/D) 52 Hz frequencies, showing color impedance and wiggle trace wavelets, respectively. Note wavelet sections have interpreted model shown behind as solid colors.

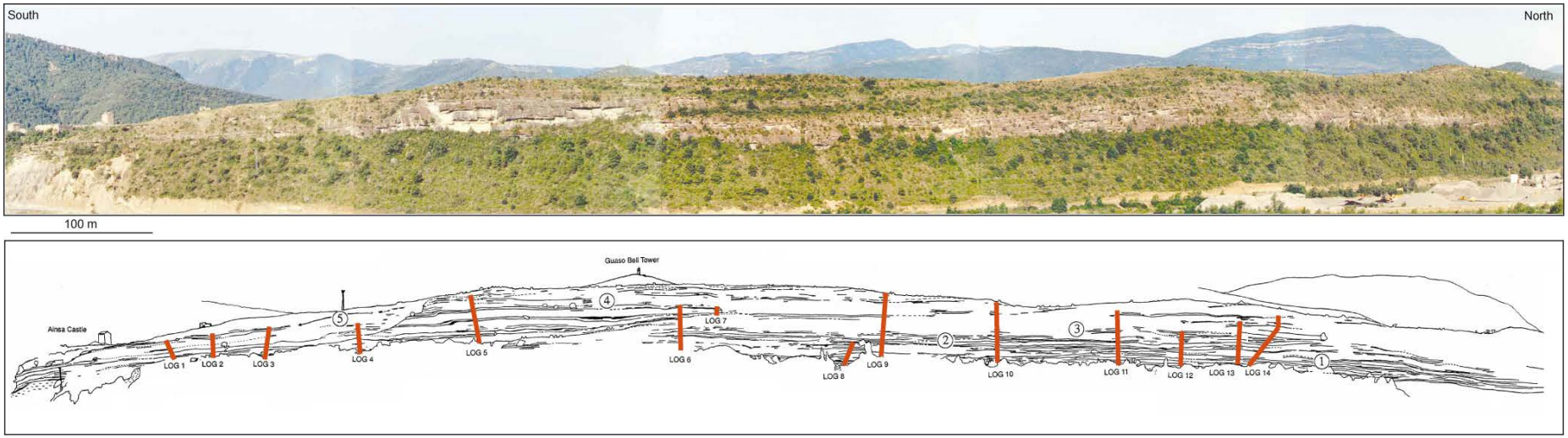

Figure A1. Photomontage and interpretation of the Ainsa II Channel Complex viewed from across the East. Sedimentary logs through the section are shown in red labeled 1 - 14. The lateral southward shifting of channel bodies can be seen in the photomontage.

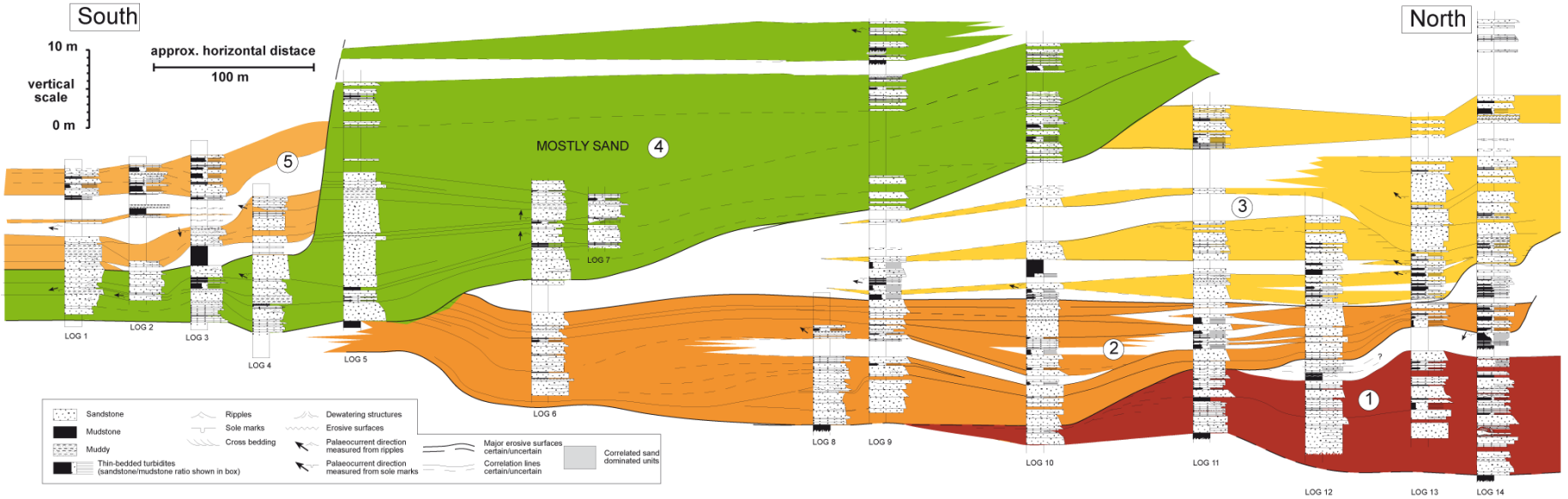

Figure A2. Bed correlation of the Ainsa II Channel showing the five stacked channel elements numbered 1-5 (adapted from Clark, 1995). See Figure 4 for log locations.

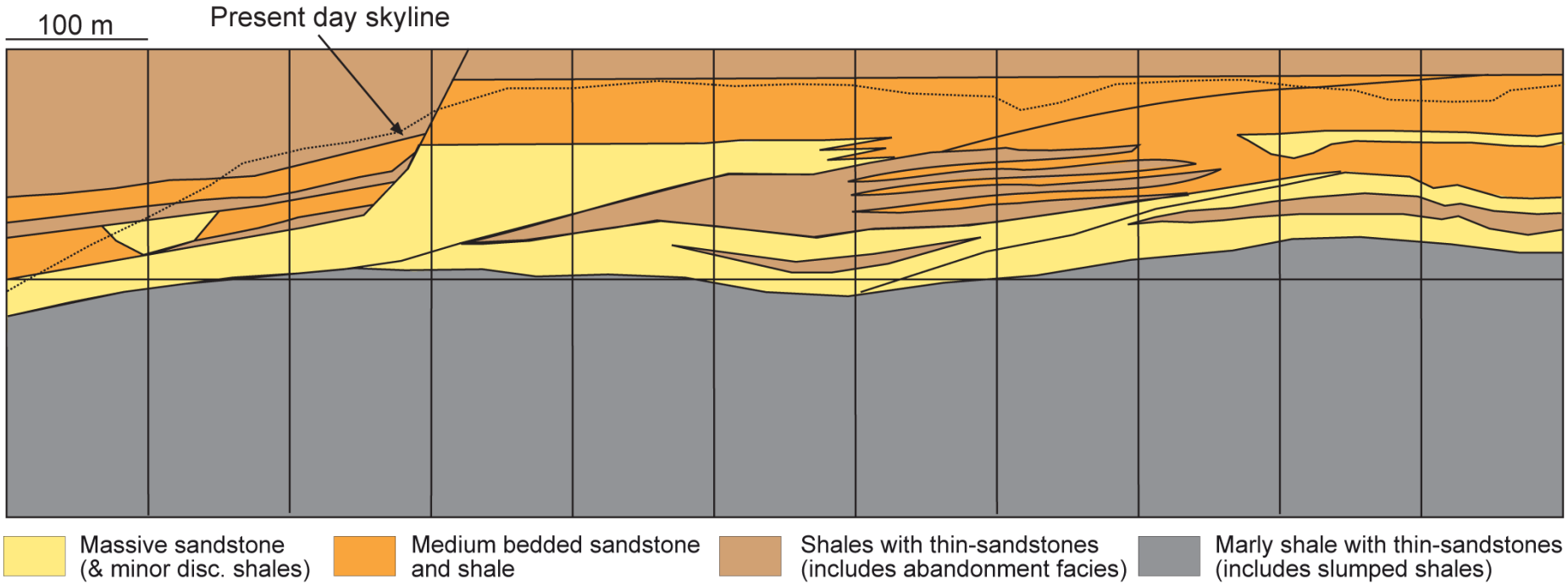

Figure A3. Sedimentary interpretation of the Ainsa II Channel Complex from a combination of photomontage interpretation, sedimentary log correlations and walking-out of key stratigraphic surfaces.

Gulf of Mexico Parameters			
	Velocity (m/s)	Density (g/cc)	Impedance ($kg\ m^{-2}\ s^{-1}$)
Massive sandstone	3672	2.08	7628×10^3
Shale and marl	2650	2.25	5692×10^3
Medium bedded sandstones & shales	3387	2.13	7214×10^3
Thin bedded sandstones & shales	2900	2.19	6351×10^3

Jurassic North Sea Parameters			
	Velocity (m/s)	Density (g/cc)	Impedance ($kg\ m^{-2}\ s^{-1}$)
Massive sandstone	4233	2.43	10286×10^3
Shale and marl	3110	2.53	7868×10^3
Medium bedded sandstones & shales	3858	2.48	9568×10^3
Thin bedded sandstones & shales	3484	2.51	8727×10^3

Figure A4. Seismic parameters used in this study.

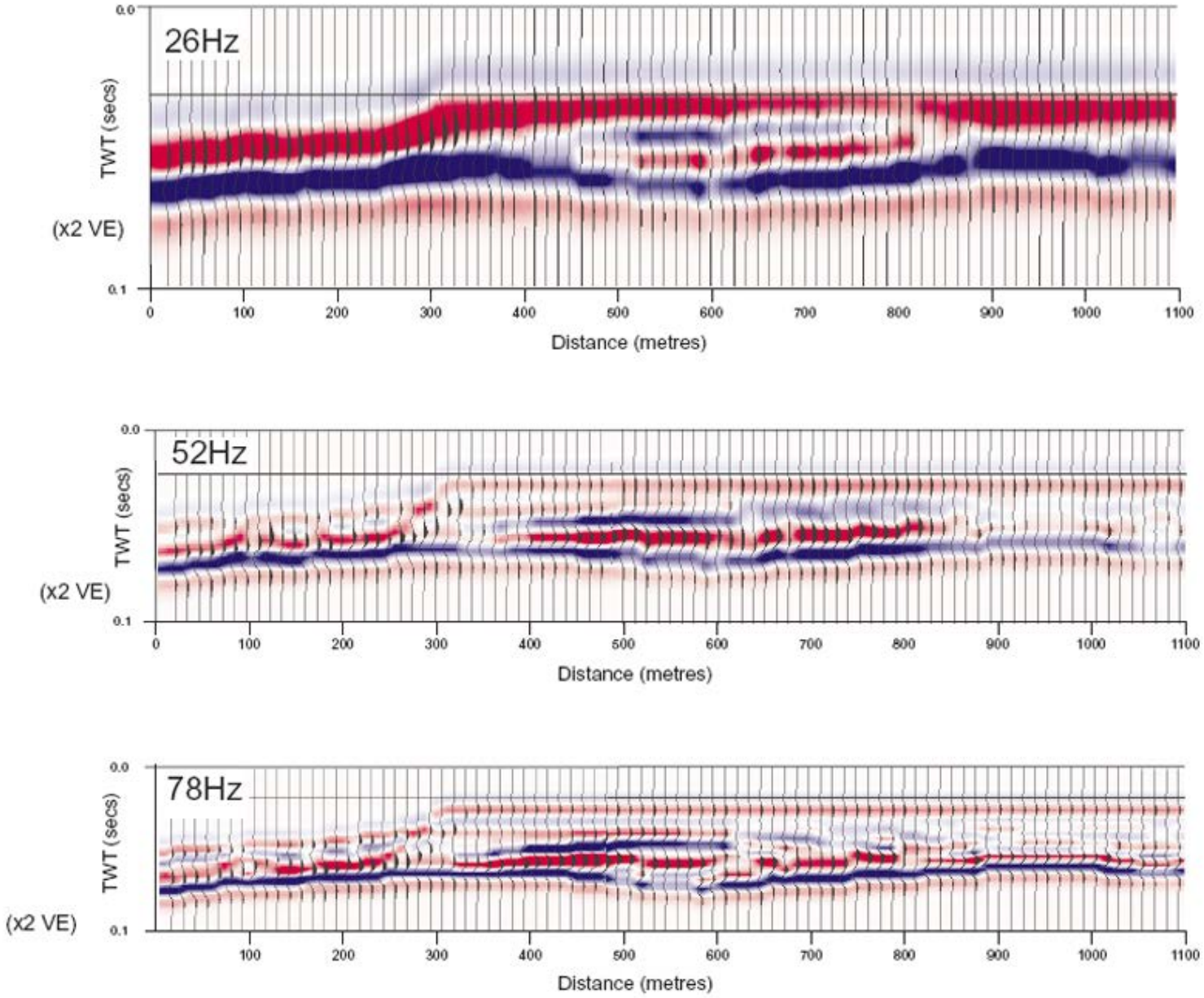

Figure A5. Plio-Pleistocene aged, Gulf of Mexico analogue output from GMAplus STRUCT™ software showing 26 Hz, 52 Hz, and 78 Hz frequencies, with both B-W-R color impedance and wiggle trace wavelets respectively (see text for description and discussion). Note wavelet sections have the input model shown behind as solid colors.

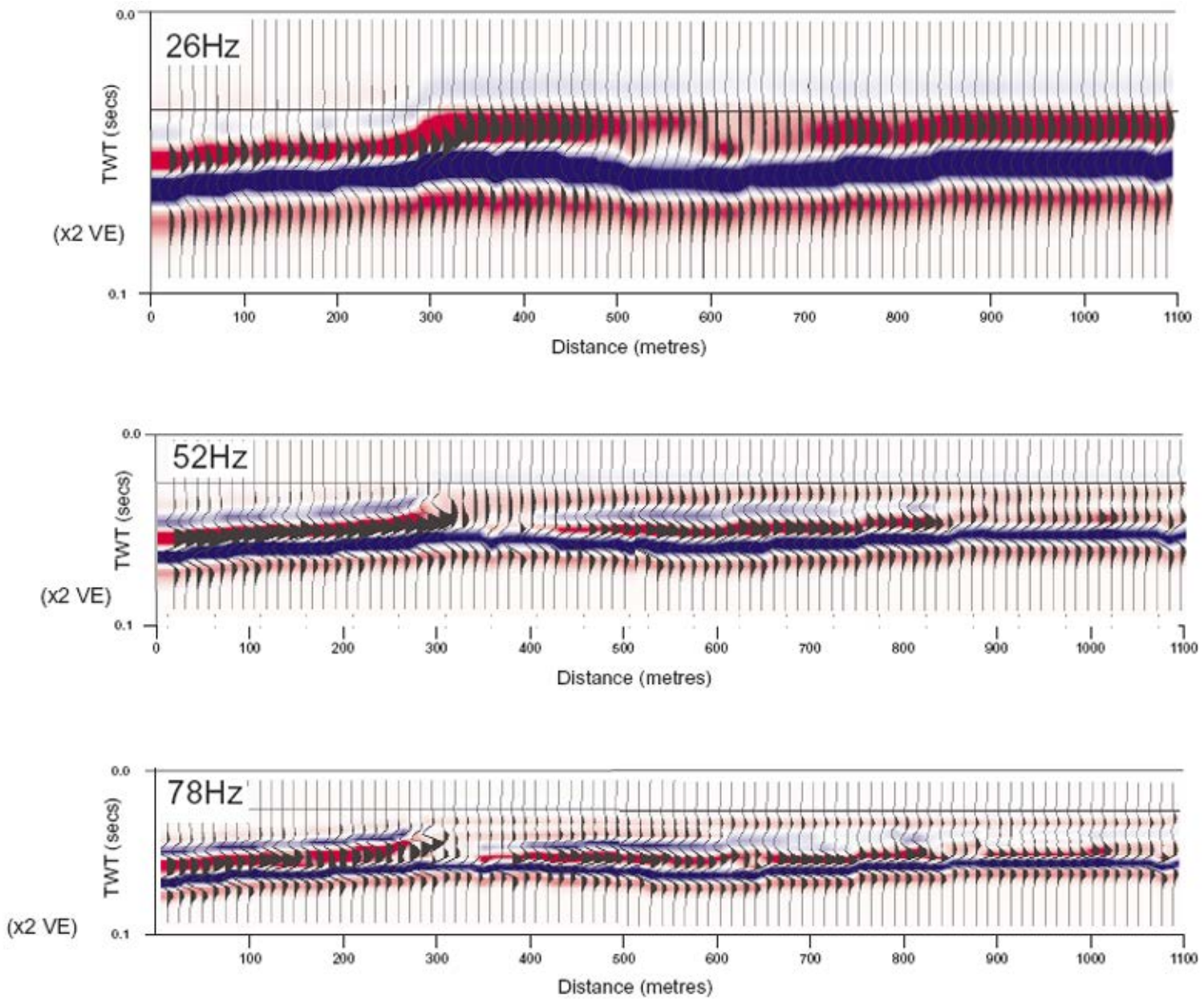

Figure A6. Jurassic aged, UK North Sea analogue output from GMAplus STRUCT™ software showing 26 Hz, 52 Hz, and 78 Hz sequences, with both B-W-R color impedance and wiggle trace wavelets respectively (see text for description and discussion). Note wavelet sections have input model shown behind as solid colors.